International Conference on Automatic Inspection and Measurement

Richard A. Brook, Michael J. W. Chen
Chairmen/Editors

Proceedings of SPIE—The International Society for Optical Engineering

Volume 557

International Conference on Automatic Inspection and Measurement

Richard A. Brook, Michael J. W. Chen
Chairmen/Editors

Cosponsored by
Sira Ltd.—The Research Association for Instrumentation
Cooperating Organizations
Optical Sciences Center/University of Arizona
Institute of Optics/University of Rochester

August 20-21, 1985
San Diego, California

Published by
SPIE—The International Society for Optical Engineering
P.O. Box 10, Bellingham, Washington 98227-0010 USA
Telephone 206/676-3290 (Pacific Time) • Telex 46-7053

The papers appearing in this book comprise the proceedings of the meeting mentioned on the cover and title page. They reflect the authors' opinions and are published as presented and without change, in the interests of timely dissemination. Their inclusion in this publication does not necessarily constitute endorsement by the editors or by SPIE.

Please use the following format to cite material from this book:
Author(s), "Title of Paper," *International Conference on Automatic Inspection and Measurement,* Richard A. Brook, Michael J. W. Chen, Editors, Proc. SPIE 557, page numbers (1985).

Library of Congress Catalog Card No. 85-062882
ISBN 0-89252-592-4

Printed in the United States of America.

INTERNATIONAL CONFERENCE ON AUTOMATIC INSPECTION AND MEASUREMENT

Volume 557

Conference Committee

Chairmen
Richard A. Brook
Sira Limited, United Kingdom

Michael J. W. Chen
Machine Intelligence Corporation

Session Chairmen
Session 1—Image Acquisition Systems and Sensors
Richard A. Brook, Sira Limited, United Kingdom

Session 2—Integrated System Design
Michael J. W. Chen, Machine Intelligence Corporation

Session 3—Information Processing
Ning-San Chang, Hewlett Packard Laboratories

Session 4—Industrial Needs and Case Studies
André Oosterlinck, Catholic University of Leuven, Belgium

INTERNATIONAL CONFERENCE ON AUTOMATIC INSPECTION AND MEASUREMENT

Volume 557

INTRODUCTION

This first conference on automatic inspection and measurement was held August 20-21, 1985 in San Diego, California, USA. Automatic inspection has become the predominant industrial application of computer vision, which has been heavily influenced by image processing, pattern recognition, artificial intelligence and robotics. This proceedings, the most significant collection of papers on automatic inspection and measurement ever assembled, accurately reflects the current state of this important integration of the robotics and computer vision technologies.

The global interest in automatic inspection and measurement for improving productivity and increasing quality is reflected in the content and origins of the conference papers. Belgium, Israel, the United Kingdom and the United States were represented. Content ranges from theoretical to practical, from micro- to macroscopic and from front-end sensing and processing of visual/force/torque/stress information to specialized parallel, high-speed, on-line architectures. Substantial effort has been put into system integration concepts, illustrating the multidisciplinary nature of the problem. There are also papers covering artificial intelligence and expert system concepts in inspection, and pragmatic methodology in angular and circularity measurements. Industrial applications vary from microelectronics, automotive, to nuclear industry, reflecting the diversity of the application areas.

Our greatest appreciation goes to all of the authors who have participated in the presentations and contributed manuscripts for publication. Thanks are also due to all the attendees whose enthusiasm made the forum a true advancement of science and engineering in artificial vision and automated inspection.

Michael J. W. Chen
Machine Intelligence Corporation

Richard A. Brook
Sira Limited, United Kingdom

INTERNATIONAL CONFERENCE ON AUTOMATIC INSPECTION AND MEASUREMENT

Volume 557

Contents

INTERNATIONAL CONFERENCE ON AUTOMATIC INSPECTION AND MEASUREMENT

Volume 557

Session 1

Image Acquisition Systems and Sensors

Chairman
Richard A. Brook
Sira Limited, United Kingdom

Development of an automated image shearing microscope for measuring the critical dimensions of magnetic recording heads.

Chris P. Kirk

Department of Electrical and Electronic Engineering, Leeds University
Leeds, West Yorkshire. LS2 9JT. England

and

Richard W. Gale

Vickers Instruments
Haxby Road, York, North Yorkshire. YO3 7SD. England

Abstract

The development of an automated image shearing microscope for measuring the lengths of the gaps in magnetic recording heads is discussed. A model is developed for a manual measurement system and this is used to identify sources of measurement error. The architecture of an automated measurement system is described in detail. Algorithms for automating the measurement process are presented and the model is extended to analyse their performance. These algorithms include a method of finding a clean site, automatic focusing and automatic measurement based on image shearing. The effects of system parameters such as illumination bandwidth, focus error and transducer resolution are investigated and it is shown that gap lengths as narrow as 0.5μm may be measured reliably. Experimental performance tests show that the system can measure gap lengths to better than 0.05μm (3σ) reproducibility in under 4 seconds.

Introduction

During the manufacture of magnetic recording heads it is necessary to be able to make precise measurements of the length of the gap in the magnetic circuit. There are many types of magnetic head currently being manufactured, but this paper is primarily concerned with measuring gaps of between 0.3μm and 3.0μm. These heads are used mostly for computer disc storage systems and video tape recorders.

Floppy disc heads have gap lengths of the order of 2μm and are often made in long blocks called loaves. These blocks are cut up into slices to form the individual heads. Most manufacturers choose to measure the length of the gap before the loaf is sliced. The allowed tolerance on floppy disc head gaps is usually about ±0.3μm, but future developments may bring this down to ±0.1μm. Audio recording heads for video recorders are made and measured in a similar manner, but generally have gap lengths of around 1μm.

Winchester disc heads are made individually and require not only the gap length to be measured but also the gap width (figure 1). The gap lengths vary from about 0.5μm to 1.0μm while the gap widths vary from about 20μm to 50μm. The allowable tolerance on the gap length is typically about ±0.1μm while the tolerance on the width is considerably greater. Magnetic heads used for the video channel in video tape recorders have the smallest lengths of all. These heads are generally made in loaves with gap lengths of between 0.3μm and 0.6μm, and a manufacturing tolerance of the order of ±0.05μm.

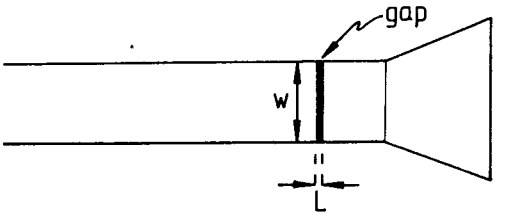

Figure 1. Top view of a Winchester head, with gap length L and width w.

Usually every head gap will need to be measured during manufacture and so a fast, reliable and low cost measurement system is required. The high precisions demanded of these measurements and the high throughputs involved, make it desirable to automate the measurement process. Even at the end of the manufacturing process each head still has a relatively low value and so measuring the gap can add considerably to the production cost.

Time consuming cleaning processes need to be avoided and so the measurement system must be able to cope with dirty heads. In order to successfully replace existing manual measurement systems, an automated system must ideally fulfill the following specification.

i) Automatically focus and measure in under 4 seconds.
ii) Measure gap lengths as short as 0.5μm to a precision of ±0.04μm (3σ).
iii) Measure gap widths (Winchester heads) of 20μm to 50μm to a precision of ±0.1μm (3σ).
iv) Be able to measure in the presence of scratches, dirt, chips etc.

The most common approach to measuring these gap dimensions is to use an optical microscope fitted with an image measuring attachment. The dimensions involved in these measurements are so small that it is necessary to consider the diffraction effects of the optical system. This measurement problem is very similar to the problem of measuring linewidths on integrated circuit photomasks. A considerable amount of work on photomask linewidth measurement has appeared in the literature[1,2] and this has been used in the design of magnetic head gap measurement systems[3]. Although much of the theoretical analysis is common to the measurement of photomask linewidths and head gap lengths, the constraints imposed by the production environments are very different.

Measurement system models

The imaging part of the measurement system consists of an optical arrangement operating with incident illumination, an image shearing device and a video camera. The system is set up for Köhler illumination and a green filter is used to restrict the illumination bandwidth (figure 2). The relative reflectivity of the glass section in a magnetic head is very low and when several heads were examined, very little reflected light was detected from this region. If the object is thus assumed to be of infinite contrast then the reflectivity a(x) for a gap of length (L) centred on the origin may be described by,

$$a(x) = \begin{cases} 0 & |x| < \frac{L}{2} \\ 1 & |x| > \frac{L}{2} \end{cases} \qquad (1)$$

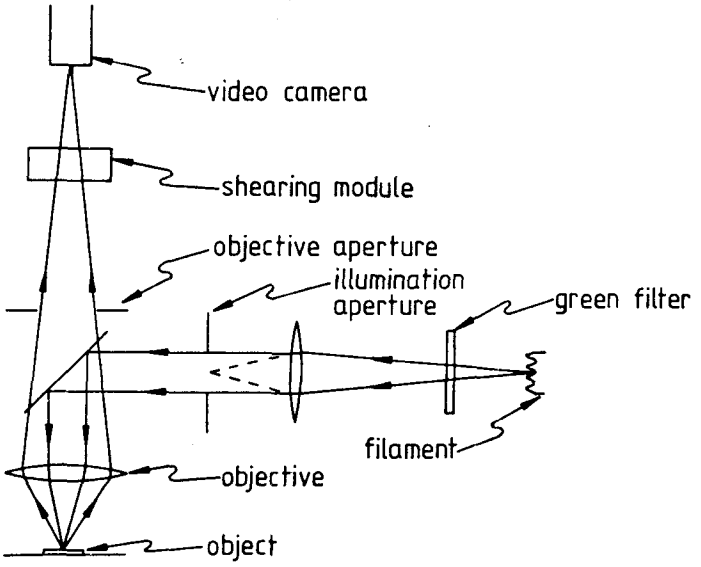

Figure 2. Schematic layout of the optical arrangement.

The gap may be treated as a one dimensional line object. This simplifies the analysis considerably as the far field diffraction pattern need only be considered in one dimension. The optical system has circular apertures and they can only be approximated to rectangular apertures when the illumination aperture is small compared with the objective aperture. Such an approximation is not valid in this case and so the image must be computed using two dimensional apertures.

If the object is assumed to be periodic with spatial frequency (b) then it may be described by a Fourier series A(q), where q is the harmonic order. The object is now described by a series of discrete spatial frequencies rather than an analytic function. Assuming that the apertures are circular then the image I(x) of the gap may be computed.

$$I(x) = \int_{-NA_c}^{NA_c} \sum_{m=-M}^{M} \left| \sum_{q=Q_1}^{Q_2} A(q).\exp(\pi ib(2qx+b\lambda\delta([\frac{\theta}{b\lambda}]^2+m^2))) \right|^2 d\theta \quad (2)$$

$$Q_1 = \frac{-1}{b\lambda}\sqrt{NA_o^2 - \theta^2} - m \qquad Q_2 = \frac{1}{b\lambda}\sqrt{NA_o^2 - \theta^2} - m \quad (3a,b)$$

$$M = \frac{1}{b\lambda}\sqrt{NA_c - \theta^2} \quad (4)$$

NA_o = objective aperture, NA_c = condenser aperture, θ = illumination angle and δ = focus error in μm.

The optical image is split into two images of equal intensity and these are displaced relative to each other by the image shearing module. Methods of shearing optical images have been discussed in the literature[4]. The image I(x) is split and displaced by an amount (p) to form the sheared image $I_s(x)$.

$$I_s(x) = 0.5\ [\ I(x+p) + I(x-p)\ ] \quad (5)$$

In a manual system the amount of shear (p) is adjusted until the opposing edges of the line object are just touching. This position is recorded (P_1) and then the images are displaced by an equal amount in the opposite direction and the images are adjusted again until the edges are aligned (P_2). The distance moved ($P_1 - P_2$) is thus a measure of twice the object length. In a correctly aligned system $P_1 = -P_2$ but in practice it is difficult (and also unnecessary) to centre the shearing mechanism accurately.

The sheared image is formed on the pick-up tube of a video camera which converts the optical image into an electrical signal. The camera introduces distortions into the image in various forms. The photometric response of the pick-up tube will not be perfectly linear. The non-linearity is usually defined by the parameter (γ) with a value of 1.0 representing a linear response. The effect of photometric non-linearity is not only to distort the image but to make the distortion a function of image intensity. The pick-up tube also has a finite resolution due to charge spreading through the photo-sensitive surface. To a first approximation the point spread function of the tube T(x) may be represented by a Gaussian response[5] which is assumed to remain constant across the tube face. The width of this response is determined by the resolution width parameter σ.

$$T(x) = (2\pi\sigma^2)^{-0.5}\ .\exp\left(\frac{-x^2}{2\sigma^2}\right) \quad (6)$$

If a raster scanned camera is used then the raster will not be perfectly linear and this will result in geometric distortion of the image. The deviation of the raster from its correct path is a function of position and can be described by the function e(x). Unfortunately e(x) is a function of temperature, time, light intensity and the electrical drive conditions of the tube. The resultant distorted video signal v(x) is given by,

$$v(x) = \left[\ c + \int_{-\infty}^{\infty} T(X).I_s(x-e(x)-X)\ \right]^{\gamma} dX \quad (7)$$

c = dark level response of the camera.

The video signal can be used to perform the edge to edge setting. The alignment is made by adjusting the shearing until the two images appear to merge into one. When this happens, the intensity profile across the aligned edges becomes flat. Since the measurement is based on the optical displacement, it is unaffected by the geometric distortion of the raster. The photometric non-linearity and resolution do not introduce any error, since the profile across the aligned edges is flat. The video signal can thus be used for performing the alignment without introducing any error.

At this point it is worth considering the problems of direct measurement from the video signal. In a typical optical microscope, the magnification of the image on the pick-up tube results in a scale of about 0.05μm per scan line. If an object is to be measured to a precision of 0.01μm then the video profile will need to be sampled at least once every 0.005μm which results in a sampling rate of about ten times the video bandwidth. This is expensive and prone to noise as well as all the forms of distortion described in equation 7.

Using the image shearing technique, not only is the camera distortion avoided but much coarser sampling is possible. When the two images are not correctly aligned, there will be either a dark fringe (under shear) or bright fringe (over shear) at the point where the two edges meet. This fringe cannot be narrower than the point spread function of the video camera and so in order to detect the presence of a fringe (and thus detect a shearing misalignment) it is not necessary to sample the profile at intervals smaller than the point spread function width of the camera. For most video cameras, the point spread function has a width of several raster scan lines and thus sampling once every scan line is more than

adequate in order to align the sheared images. This would represent a reduction in the sampling rate of a horizontal scan of about a factor of 10. However since the image need not be sampled more often than once every scan line, the image may be sampled vertically by sampling the video profile at the same distance along each scan line. Thus the image is now sampled at line scan frequency which is about 2,500 times slower than the sampling necessary to perform a direct video measurement. In addition it is possible to take advantage of the fact that the gap is a one dimensional object and thus the intensity along each horizontal scan should be constant. This means that the video signal can be sampled over a long interval and so reduce the effects of noise.

Architecture of the measurement system

The main structure of the measurement system is shown in figure 3. The system is controlled by a microcomputer which handles the capture of the image profiles and the adjustment of the stage height and shearing mirror. The positions of both the shearing mirror and the stage are detected using strain gauges mounted on flexure springs. The output of these gauges is extremely linear and stable with temperature and so it provides a precise indication of position. In order that a low cost microcomputer could be used, the control of the stage and shearing position is performed by analogue control loops rather than the computer. Both the stage and shearing mirror are driven by motors which are controlled by compensated integrating feedback loops (figure 4). These loops enable the stage and shearing mirror to accurately track the positions demanded by the digital to analogue converters connected to the computer.

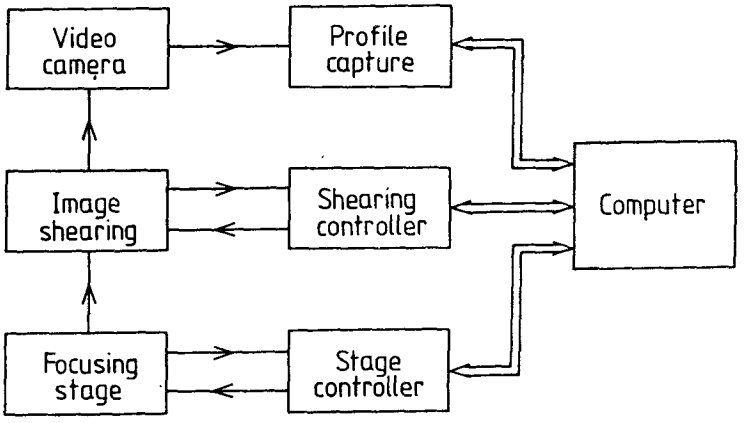

Figure 3. Measurement system block diagram.

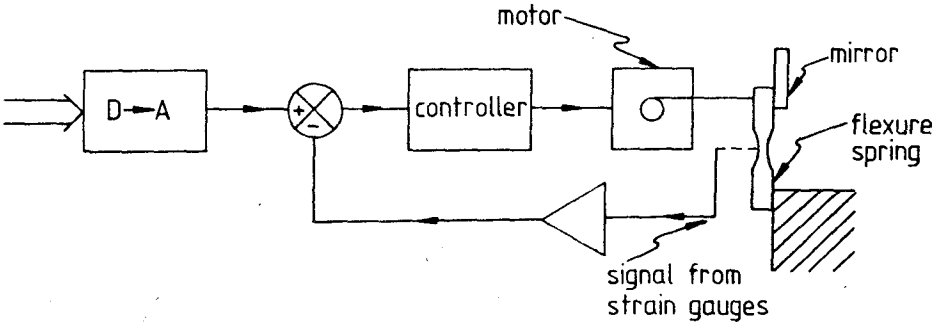

Figure 4. Layout of the control loop for adjusting the shearing mirror. The control loop for the the focusing stage has a similar configuration.

The measurement technique does not require rapid sampling of large amounts of data and this has helped to keep the cost down. The video image is sampled at the same distance along each line scan (figure 5). The sampling position T_1 is controlled from the computer and this cursor may be moved across the screen under software control. After time T_1 along each scan line, a sample and hold samples the image for time ΔT and then holds this value until the start of the sample period on the next line. At the end of the period ΔT, when the signal has been captured, an 8 bit analogue to digital conversion is initiated and the value transferred to the microcomputer.

In order to perform the measurement correctly it is necessary to be able to position the head gap parallel to the raster scan lines. This is achieved by a K-prism in the optical

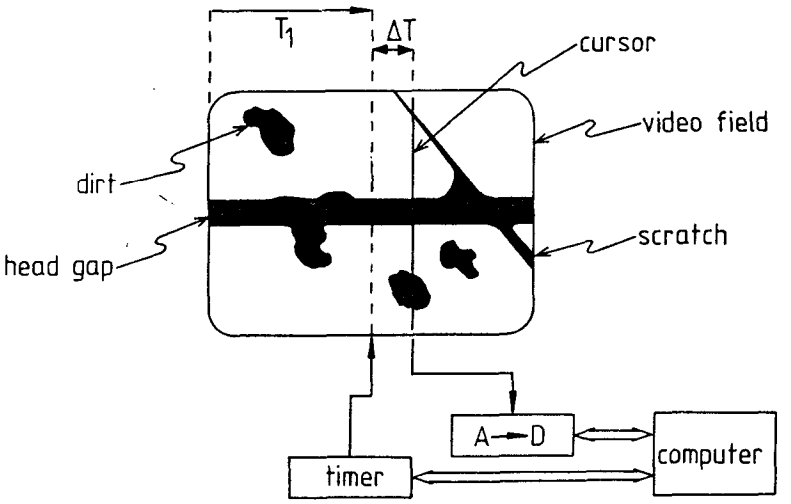

Figure 5. Video field of a gap in a magnetic head with dirt and scratches. The cursor position determines the location of the sampling window.

path which rotates the image. The rotating prism may be positioned by hand or using a stepper motor driven from the software. This rotation facility can also be used to turn the image through 90°, which enables both gap lengths and widths to be measured without moving the heads on the stage.

The automatic focusing is based on the steepest slope method and takes place in two stages. The object is stepped coarsely through the focus range of 30μm and the image profile is captured at each step. Each profile (I(n)) is filtered with an M element slope detecting filter (f(m)) to produce a signal ($I_f(n)$) with an amplitude which is focus sensitive.

$$I_f(n) = \sum_{m=0}^{M} I(n+m).f(m) \qquad (8)$$

The stage position where the peak value of $I_f(n)$ was at its greatest is taken as being the nearest to the focal plane and the object is returned to this position. The scanning and filtering is then repeated but with smaller steps and over a smaller range about the approximate focus position. The stage position generating the greatest filter response from this second scan is taken as being the critical focus and the object is returned to this position. The complete focusing operation takes about 2 seconds to locate the focal plane from anywhere within the 30μm range. However when moving along a loaf or when coarse manual focusing is used, only the fine focusing is necessary and this reduces the time taken to less than 0.5 seconds.

The heads are dirty, scratched and chipped and so it is necessary to find a clean area in which the measurement can be performed. After the focusing operation is complete, a clean site finding routine is initiated. The sampling line is moved through 16 positions across the field of view and the image profile is capture at each site. All these profiles are then added together to form a mean profile. The head gap is a continuous feature across the field of view and so all the profiles will contain a dip corresponding to the position of the gap. Thus when added together, the mean profile will also contain a dip at the position of the gap. The different profiles will contain dips due to dirt and scratches, but these will be in different positions in different profiles. Thus when the profiles are summed, the scattered dips due to dirt and scratches will reduce in amplitude as they are not common to all the profiles. The summed profile will thus contain one large dip due to the head gap and a series of small dips due to dirt and scratches.

The position of the head gap is now located from this profile. The lowest (I_g) and highest (I_m) intensity values are detected in the profile and the intensity of the line edges (I_e) is defined as the mean of these two values. Starting at the element in the image array with the lowest value (I_g), the array is examined in both directions until the intensity rises to I_e. The positions where this intensity is crossed (X_1,X_2) are taken as the line edges and the central position of the gap (X_c) is defined as the mean of X_1 and X_2. This algorithm enables the gap to be located rather than dirt or a scratch.

Some dirt, chips and scratches will lie across the head gap and so measurement at these sites must be avoided. If any of these artefacts lie at the edge of the gap, then they will cause the gap to appear longer at that site than it should be. Each of the 16 profiles is

examined in turn and the length of the gap at X_c is determined by locating the points X_1 and X_2 corresponding to the threshold I_e. The profile which contains the shortest gap is assumed to lie at the cleanest site. The algorithm has now located the gap and the best position along it for measurement.

The measurement algorithm relies on detecting edge to edge shearing alignment by digitally filtering the sampled sheared image profile[6]. Once the measurement site has been located, several image profiles are captured and summed. This gives a low noise sampled profile of the site before shearing. Using the I_e definition of the edge threshold, the approximate gap length is calculated and the shearing is adjusted by an amount just short of this value. In order to exclude artefacts other than the two edges being aligned, the profile signal is windowed to cover only a region of ±1/2 a gap length on either side of the gap centre location (X_c). The profile will now take the form shown in figure 6. In order to align the edges, the images are stepped through from the under shear to the over shear condition and at each step a profile is captured, windowed and filtered (equation 8). If a high pass filter is used then the filtered signal $I_f(n)$ will have a minimum response when the opposing edges of the gap images are aligned. The high pass filter may take the form of a slope sensitive filter (eg. [-1,1] or [-1,0,1]) or a curvature sensitive filter (eg. [-1,2,-1] or [-1,0,2,0,-1]). Both the models described earlier and empirical results show that the curvature rather than the slope sensitive filters are better for locating the aligned edges condition.

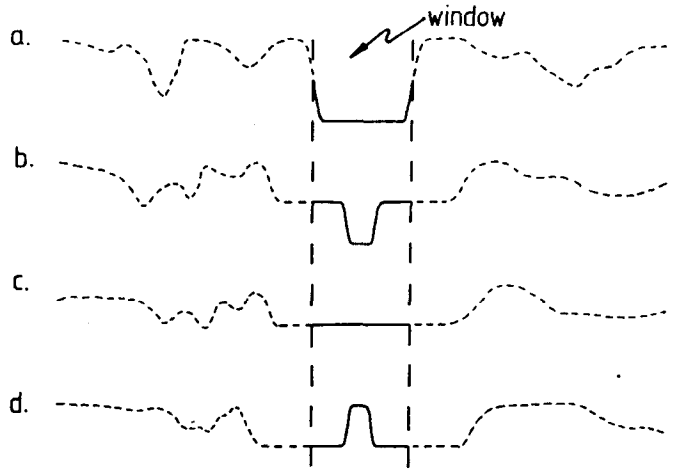

Figure 6. A window is located in the unsheared image profile (a) between the two edges, and the profile filtering is restricted to this region. Curves b,c and d show the under, exact and over shear conditions respectively.

Theoretical study of system performance

The model described earlier was developed to enable the effects of various parameters in the optical system to be determined. The system described in the last section produces a precise measurement and it is necessary to relate this to an actual accurate value. The model will enable these systematic errors to be identified and quantified.

A 0.85 NA objective was used with the illumination source filling the back aperture. The system magnification resulted in an image scale on the pick-up tube of 0.03μm between the raster scan lines and a resolution width parameter (σ) of 0.06μm. Different edge detection filters were used but it was found that a [-1,0,0,2,0,0,-1] array produced the most sensitive response.

When the gap length becomes comparable with the resolution limit of the system, the image profiles will distort and this will affect the measured value. A range of gap lengths from 0.5μm to 3.0μm were examined (figure 7a) and it was found that the measured gap length was consistently 0.12μm wider than the true value. This makes the calibration procedure relatively simple. The shearing movement may be calibrated from a stage micrometer and then all the measurements can be corrected by subtracting this offset.

The steepest slope method of automatic focusing is capable of locating the focal plane to within ±0.2μm. A theoretical investigation of the effect of focus errors (figure 7b) showed that focus errors of up to ±0.5μm produced measurement errors of only ±0.01μm. Since the object field profile is real and symmetrical, the effects of defocus are the same in either direction. The focusing mechanism is thus adequate for the measurement precision required.

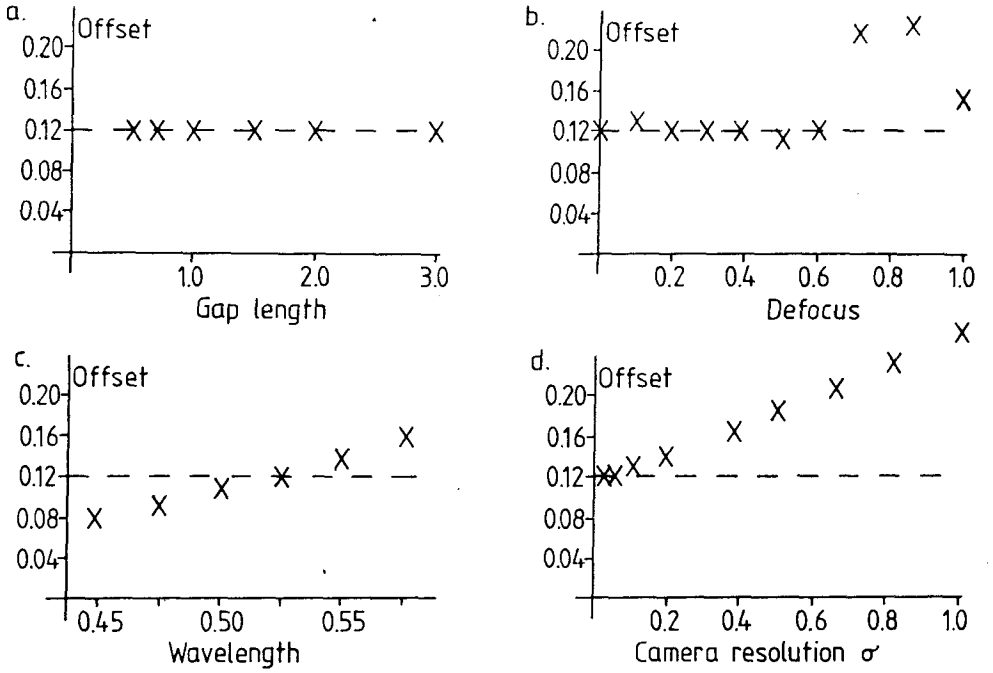

Figure 7. The theoretical offset between the measured and actual gap length as a function of gap length (a), defocus (b), wavelength (c), and camera resolution width (d).

The image edge slope is a function of illumination wavelength and this will affect the gap length measurement (figure 7c). Short wavelengths produce images with sharp edges and so the gap length measurement offset should decrease with wavelength. The theoretical edge profile produced by the broadband green filter is very similar to the profile produced by monochromatic green light (λ = 0.53μm). However work by Nyyssonen[1] suggests that the image edge profile is more sensitive to illumination wavelength because of chromatic aberrations which have been ignored here. In practice it was found that the measurement technique used was insensitive to illumination bandwidth. Measurements performed using a green filter were found to agree with those using white light, to within 0.01μm.

The effective camera resolution (σ) is determined by the magnification on the tube face. Figure 7d shows how this effects the gap length measurement offset on a 2.0μm long gap. The system described in the last section has a σ of 0.06μm and according to the model this introduces a measurement error of only 0.01μm on gap lengths as short as 0.5μm. Increasing the magnification would allow smaller gap lengths to be measured without incurring a larger measurement error. The effect the camera has on the measurement offset depends on the gap length. As the gap becomes shorter it is no longer small compared with the resolution width (σ) of the camera and so the outer edges of the sheared line image will distort the image profile and introduce a measurement error.

Experimental verification of system performance

Experimental results were obtained using batches of Winchester and floppy disc magnetic heads. The system was first operated in its manual mode in order to provide a reference to compare with the automated performance. Four operators each measured a nominally 1.8μm floppy disc head gap 25 times. The 3σ reproducibility varied between 0.03μm for an experienced operator and 0.05μm for an inexperienced operator. However although the operators achieved very good reproducibilty individually, when their measurements were compared the agreement was not quite as good. The four operators achieved 3σ reproducibilities of 0.03,0.04,0.04 and 0.05μm individually, but collectively the 3σ reproducibility was 0.06μm. Thus each operator judges the focus and edge setting conditions differently and one advantage of automation is that it eliminates this element of subjectivity.

In order to assess the precision of the measurement technique, the system was carefully focused manually using an optical precise focus indicator[7]. 25 automated gap length measurements were performed on each head and the 3σ reproducibility values obtained lay between 0.025μm and 0.035μm. The 3σ reproducibility of the manual measurements performed at the same sites by an experienced operator varied from 0.035μm to 0.045μm. Thus the automation of the measurement represents a significant improvement in reproducibility. The

measurements were repeated but allowing the system to focus automatically. The 3σ reproducibilities now varied from 0.027μm to 0.048μm (with a mean of 0.036μm). This is an improvement over the manual measurements.

In order to investigate the relationship between these gap length measurements and accurate values, several of the heads were examined in a scanning electron microscope (SEM). The gap length varied along the head by about ±0.03μm and it could not be guaranteed that the optical and SEM measurements were being compared at exactly the same site. Despite this, the measurements from the SEM pictures suggested that the optical measurements were between 0.04μm and 0.08μm larger than the true gap length. According to the theoretical model described earlier, this offset should be 0.12μm. When calculating this offset, it was assumed that the glass did not reflect any light. In fact the theoretical reflectivity of the glass is about 4% and when this is included in the model, the theoretical offset between the true gap length and the measured value falls to 0.06μm. This agrees well with the value obtained from comparing the optical measurements with the SEM pictures.

The measurement of gap widths is a lot easier as they are much wider and the measurement precision required is less exacting. On a batch of Winchester heads, the system achieved 3σ reproducibilities of between 0.04μm and 0.07μm on gap widths of between 20μm and 50μm.

Conclusion

An automated critical dimension measurement system has been developed for measuring the length and width of the gaps in magnetic recording heads. A complete focusing and measuring cycle takes about 4 seconds with an overall 3σ reproducibility of under 0.05μm (gap lengths). The system is also capable of automatically locating clean measurement sites.

Acknowledgements

The authors would like to thank Val Burke for providing information for the specification of this instrument and Derek Moore for the design of the shearing and stage movements. The work has been funded by the Science and Engineering Research Council and Vickers Instruments.

References

1. Nyyssonen, D., "Linewidth Measurement with an Optical Microscope: The Effect of Operating Conditions on the Image Profile", Appl. Opt., Vol.16, 2223 (1977).
2. Jerke, J.M., "Accurate Linewidth Measurements on Integrated-Circuit Photomasks", NBS Special Publication, 400-43, (1980).
3. LeMaster, R.J., "AIM - An Automated Inspection Microscope for Measuring Critical Dimensions", Proc. Soc. Photo-optical Instrum. Engrs. 480 Integrated Circuit Metrology II, 40-48 (1984).
4. Smith, F.H., "Binocular Image-Shearing Microscopes", Advances in Optical and Electron Microscopy, Vol.9, Academic Press, London and New York (1984).
5. Kirk, C.P., Moore, D.S. and Nelson, J.C.C., "Analysis of Linewidth Measurement Techniques for the Purpose of Automation", Proc. Soc. Photo-optical Instrum. Engrs. 480 Integrated Circuit Metrology II, 33-39 (1984).
6. Kirk, C.P., UK. Patent Application No.8507843 (1985).
7. Smith, F.H., UK. Patent Application No.8016517 (1980).

Design of Robot Hand-Based Intelligent Sensor for Measuring Six DOF Force/Torque Information

Ren C. Luo

North Carolina State University
Department of Electrical and Computer Engineering
P.O. Box 7911, Raleigh NC 27695-7911

Michael J. Chen

Machine Intelligence Inc.
330 Potrero Ave., Sunnyvale, CA 94086

Abstract

The objective of this paper is to describe the design of a pair of sophisticated robot fingers which enable to sense three axis of forces and three axis of torques information using piezo-resistive strain gauges as sensing elements with frequency output. The fingers may be mounted onto a servo controlled robot gripper and interfaced with robot controller to serve as active compliance device for small parts assembly tasks. This newly direct force/torque sensor with frequency output employing RC oscillation principle has demonstrated great advantages with signal conditioning and processing relative to the conventional voltage output procedures. A description of the test results is also presented.

Introduction

A major challenge in the development of intelligent robot systems is the acquisition and use of sensory information such as visual, tactile, force/torque and other types of sensors for motion feedback control.

The required sensors to extend the capabilities of the roobot can be grouped basically in three areas; 1) those needed prior to contact (vision, range, proximity sensors); 2) during contact (touch, slip sensors). Force/torque sensors usually mounted between the end-effector and last wrist joint provide information on the amount of force and torque exerted by the end-effector on objects along three orthogonal directions referenced to the end-effector [1, 2].

The application of industrial robots in manufacturing has been proven successfully in broad areas, however, it is still rather deficient in the area of assembly. The deficiency stems from a lack of sensory capability to cope with the compliant characteristic embedded in the assembly task. Robotics applications in the area of assembly automation has attracted great research efforts. Methods for improving robot capability in accomplishing the assembly task can be generally divided into two groups, i.e. active compliance and passive compliance. In active compliance, robot compensatory motion is provided by a servo actuation system whose decision is dependent on the information extracted from some form of sensory feedback and the control algorithm. Compliance flexibility and programmability can be obtained to suit the assembly task [3 -5]. In passive compliance, where compliance is provided by structural nature of the robot, or by a special device which offers fixed mechanical compliance for a particular task, for example, the remote center compliance (RCC) used for insertion tasks [6, 7].

Typical assembly tasks such as inserting a peg into a hole using robots have been studied to a great extend [8, 9]. However, such solutions commonly assume the rigidi ty of the parts in contact and a restriction to single pin insertion. In addressing assembly problems in general, those involving small electronic components are of particular interest.

The objective of this paper is to describe the design of a pair of sophisticated robot fingers which enable to sense three axis of forces and three axis of torques information while the robot performs the insertion of several pins (e.g. IC chips) into holes with tight tolerance. Because of the leads are deformable, the compliance varies, so that a passive compliance concept would not be suitable. An active concept will then be needed. First some brief discussions on the nature of force/torque fingertip sensors will be offered. Then, description will be presented which covers the design criterium, signal conditioning and processing, and data acquistion systems, as well as its performance. Finally, some of the test results will also be presented.

Design Concept

This multi-axis force/torque sensitive fingers is considered to mount onto the previously designed servo-controlled gripper [10]. The gripper is designed parallel-jaw type with prarallogram finger structure. It is a microprocessor based servo-controlled system which consists of force and position feedback capabilites

In order to handle a variety of small parts for assembly which are non-rigid, fragile in common, several design criteriums need to be considered]11].

1) The sensor should be sensitive, accurate and reliable, since the workpiesces are small, fragile and non-rigid in common.

2) The sensor should be located as close to the object as possible. To detect the force/torque information use conventional wrist sensors may not be accurate since the sensory information are not detected from the force/torques applied to the object directly.

3) The sensor should provide multi-axis force/torque information to accomodate fine robot motion.

4) The size of the fingers should be relatively small to reduce the inertia error problem.

Mechanical Structure of the Fingers

As it is easy to measure bending moment applied to a cantilever beam, the structure of the fingers are constructed as shown in Fig. 1.

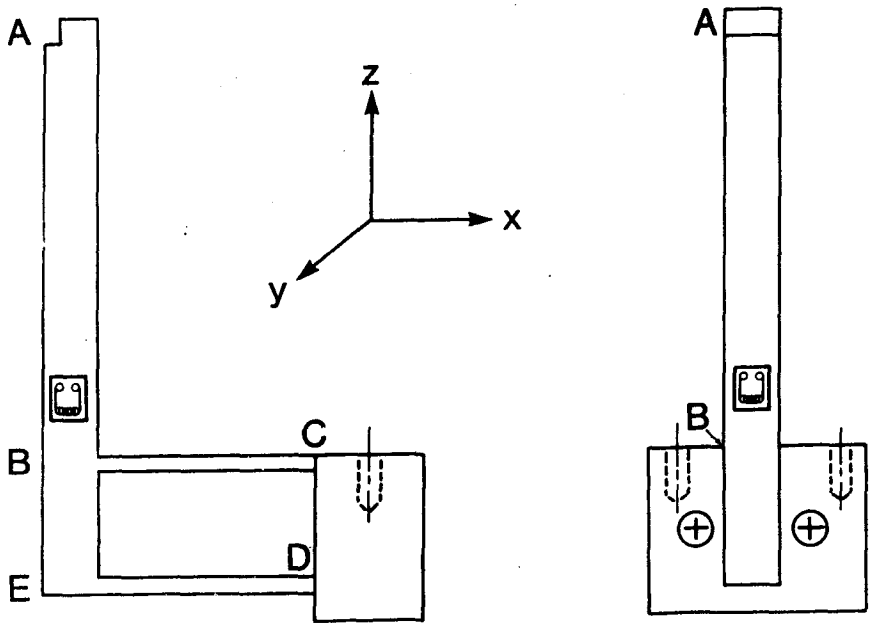

Fig. 1. Mechanical Structure of the Finger

The following is an analysis for the design of fingers. The A-B segment of the fingertip is a cantilever beam relative to the rest of the part, and the forces that are applied in the X-Y plane twisting the beam into moment. Thus strains which are proportional to the applied force can be detected near the base of the beam.

The web part BCDE of the fingertip simply detects forces in the Y-direction. The two beams, BC and ED, are supported at both ends. When a force in the Y direction is applied, a moment results on each end of the beam. Thus the strain near the ends of the